METHODS: A Companion to Methods in Enzymology 18, 215–221 (1999)
Article ID meth.1999.0774, available online at http://www.idealibrary.com on IDEAL®

Detecting Action Potentials in Neuronal Populations with Calcium Imaging

Diana Smetters, Ania Majewska, and Rafael Yuste[1]

Department of Biological Sciences, Columbia University, 1212 Amsterdam Avenue, Box 2435, New York, New York 10027

The study of neural circuits requires methods for simultaneously recording the activity of populations of neurons. Here, using calcium imaging of neocortical brain slices we take advantage of the ubiquitous distribution of calcium channels in neurons to develop a method to reconstruct the action potentials occurring in a population of neurons. Combining calcium imaging with whole-cell or perforated patch recordings from neurons loaded with acetoxymethyl ester or potassium salt forms of calcium indicators, we demonstrate that each action potential produces a stereotyped calcium transient in the somata of pyramidal neurons. These signals are detectable without averaging, and the signal-to-noise is sufficient to carry out a reconstruction of the spiking pattern of hundreds of neurons, up to relatively high firing frequencies. This technique could in principle be applied systematically to follow the activity of neuronal populations *in vitro* and *in vivo*. © 1999 Academic Press

Key Words: networks; multiunit; slices; cortex.

Current understanding of the processing of information in the nervous system is based on the piecemeal reconstruction of the function of certain circuits, after detailed analysis of the responses of single neurons to a particular stimulus. These traditional single-cell approaches have been extremely fruitful in elucidating particular neuronal pathways and have generally resulted in feedforward models of neural circuits (1–3). Recently, the field of artificial neural networks has suggested an alternative computational strategy that nervous systems may use: a feedback neuronal network (4). These network models consist of distributed circuits in which a given neuron is connected to many or most other neurons in the network, thus maximizing the distribution of information (5). To properly distinguish between these, or other, types of circuit models, it is necessary to characterize the circuit dynamics by reconstructing the activity of the network (6).

A direct approach to reveal the circuit dynamics is the use of multielectrode recordings. For example, in the retina microelectrode arrays permit the simultaneous recordings of dozen or hundreds of neurons (7). This approach, and particularly recordings with few electrodes, has the disadvantage of sampling only a small proportion of the neurons in a given area. Extracellular electrical recordings also lack anatomical information about the particular cells responsible for the spikes. If different types of neurons have different functions in the circuit, as is predicted by the apparently strict relation between morphology and function (8), then precise anatomical information is essential for a complete understanding of the circuit activation patterns.

An alternative approach to characterize circuit dynamics is optical recording from neuronal populations (9). The optical nature of the experiment permits simultaneous recording from many neurons, makes the technique noninvasive, and gives it a temporal resolution limited only by the time course of the optical event being monitored and a spatial resolution limited only by the size of the signal and the wavelength of the light used. The use of optical methods for detecting neuronal activity started with the monitoring of intrinsic signals (10, 11). Intrinsic signals suffer the disadvantage that their low signal-to-background ratio makes them ill suited for recording with single-cell resolution. A solution to this limitation was the development of indicator dyes. Two different types of dyes have been successfully used: voltage-sensitive dyes (VSDs) (12) and ion-sensitive dyes (13). VSDs were pioneered because the ideal indicator should translate membrane potential

[1] To whom correspondence should be addressed. Fax: (212) 865–8246. E-mail: rafa@cubsps.bio.columbia.edu.

1046-2023/99 $30.00

into an optical signal. Unfortunately, currently available VSDs have small signals, i.e., ~1% change in fluorescence or transmitted light in experiments done in slices or *in vivo* (14, 15). This makes single cell resolution studies possible only in cultured neurons (16). Indeed, in our work using neocortical slices, we have found that VSDs do not enable single-cell resolution recordings (17).

In contrast, optical monitoring of the activity of a neuronal population is feasible with calcium indicators (18–21) because they produce large signals (up to 1000% changes in fluorescence), making it possible to measure the responses from single neurons (22), presynaptic terminals (23), or even dendritic spines (24). In addition, development of bulk loading methods, exploiting the intracellular deesterification of acetoxymethyl ester derivatives of the indicators, enables the noninvasive loading of an entire population of neurons (25). Finally, an unexpected bonus of calcium imaging experiments has been the ability to detect electrical events by optically monitoring changes in $[Ca^{2+}]_i$. The ubiquitous presence of calcium channels in neuronal membranes and their activation by depolarization have made possible the optical detection of (i) subthreshold EPSPs, which can produce calcium influxes localized to a single dendritic spine (24), (ii) sodium action potentials, which can produce generalized calcium accumulations throughout the cell, due to the backpropagation of the spike (24), and (iii) calcium spikes, which can produce generalized calcium influxes that are much larger than those produced by sodium spikes (26). Thus, it is possible to detect whether a neuron fired an action potential by monitoring its $[Ca^{2+}]_i$ (24, 27), and since the amount of calcium influx per spike is constant (28), it should in principle even be possible to distinguish how many spikes triggered those accumulations.

Building on this previous work, we now explore the detection of the spiking activity of a population of neurons using loading of neuronal circuits with AM calcium indicators and calcium imaging. Our experiments compare the responses of neurons loaded with AM calcium indicators with those of neurons filled with calcium indicators using whole-cell patch pipets. We focus our work on the rat somatosensory and visual cortex and use coronal brain slices to easily access these circuits.

DESCRIPTION OF METHOD

Loading Neuronal Populations in Slices with AM Calcium Indicators

Slices and hemispheres were taken from postnatal day (PND) 9–20 Sprague–Dawley rats. Animals were anesthetized by hypothermia or Ketamine–Xylazine injections (ip) and the brain was removed and placed into cold ACSF (126 mM NaCl, 3 mM KCl, 26 mM $NaHCO_3$, 1 mM $NaH2PO_4$, 2 mM $CaCl_2$, 1 mM $MgSO_4$, 10 mM dextrose, bubbled with 95% O_2/5% CO_2). The somatosensory or visual cortex was manually blocked with a razor blade and a vibratome was used to cut 300- or 400-μm-thick sections. Slices were kept in a submerged incubation chamber at room temperature (~22°C). After 1 to 5 h in the incubation chamber, slices were transferred to a staining chamber, consisting of a small vial with a carbogen line, where they were stained with calcium indicators.

Previously we found that diluted solutions of AM esters load large populations of cells in developing cortex, but the labeling becomes more difficult with increasing age of the animal (19). After experimenting with different loading protocols, we found that concentrated dimethyl sulfoxide (DMSO) solutions of the AM indicators help in loading slices from older animals (29). Our current protocol is to load slices with either Fura 2-AM, Calcium Green 1-AM, or Oregon-BAPTA Green 1-AM (all dyes from Molecular Probes, Eugene, OR) using a double-incubation protocol: (i) an initial incubation with 2 μl of a 1 mM dye (in 100% DMSO) solution for 2 min and then (ii) a second incubation in 3 ml of oxygenated 10 μM dye in ACSF for 30 min. This protocol produces reliable loading of Ca^{2+} indicators in cortical slices from rats and mice as old as PND22 (Fig. 1).

Calcium Imaging and Electrophysiology

After 15 to 30 min, labeled slices were placed in a submerged recording chamber mounted on the stage of a BX50 upright microscope (Olympus). Images of filled cells were taken with a cCCD camera (Micromax, Princeton Instruments) equipped with a EEV 512 frame transfer chip (Kodak). Camera frame rates were typically 50–200 Hz and each pixel was digitized at 12 bits. Images were acquired, stored, and analyzed using a Macintosh 7100 (Apple Computers, Cupertino, CA) computer and IPLab software (Signal Analytics). Further analysis was carried out with IDL (Research Systems). For Fura 2-AM imaging, recordings were made at 340 and 380 nm excitation at the beginning and end of every experiment to assess the approximate $[Ca^{2+}]_i$ and thus monitor the health of the cells. Some experiments were carried out at the isosbestic excitation of 360 nm. For Calcium Green and Oregon-BAPTA Green, imaging was carried out at 485 nm excitation. Optical filters were obtained from Omega Optical. For Fura-2 potassium salt recordings (380 nm excitation), we defined the fluorescence change over time as $\Delta F/F = (F_0 - F_1)/(F_0)$. For analysis of the AM loaded data we defined $\Delta F/F = [(F_0 - B_0) - (F_1 - B_1)]/(F_0 - B_0)$. For Calcium Green or Oregon-BAPTA Green recordings, we inverted the sign of the $\Delta F/F$. Photomultiplier imaging was carried out with a scanning confocal mi-

croscope (Fluoview, Olympus), using a PMT (Hamamatsu R3896) and Fluoview Software (Olympus).

Pyramidal neurons were identified morphologically using differential interference contrast (DIC) microscopy and fluorescence images. Whole-cell patch-clamp recordings were performed using 3- to 7-MΩ pipets filled with intracellular solution containing (mM) 120–150 potassium gluconate, 0–20 KCl, 4–10 NaCl, 10 Hepes, 0–50 MgATP, and 0–0.1 EGTA. Nystatin stock (46 mM, 1 mg/ml in Me_2SO; Sigma) was prepared before each experiment, stored at room temperature in a lightproof container, and used for up to 6 h after preparation. A gigaohm seal was formed by pressing the pipet gently against the soma of a neuron and providing light suction. Whole-cell recordings developed within 1–5 min of making a seal, with access resistances between 10 and 20 MΩ. The amplifiers (Axopatch 200B or Axoclamp 2B, Axon Instruments) were then switched to current-clamp mode. In all experiments, potentials were recorded at room temperature and, when necessary, current was injected to keep the resting potential at approximately −65 mV. The potential was filtered at 1 kHz, digitized, stored, and analyzed using Igor (Dr. R. Bookman's macros) and an A/D board (Instrutec).

Estimation of the Concentration of Indicator Loaded

To estimate the amount of free indicator present in neurons loaded with Fura-2-AM using the above mentioned protocol, we patched a neuron in a field of Fura 2-AM loaded cells, and filled it with 50 μM potassium salt of Fura-2 (Fig. 1D). In previous experiments, we

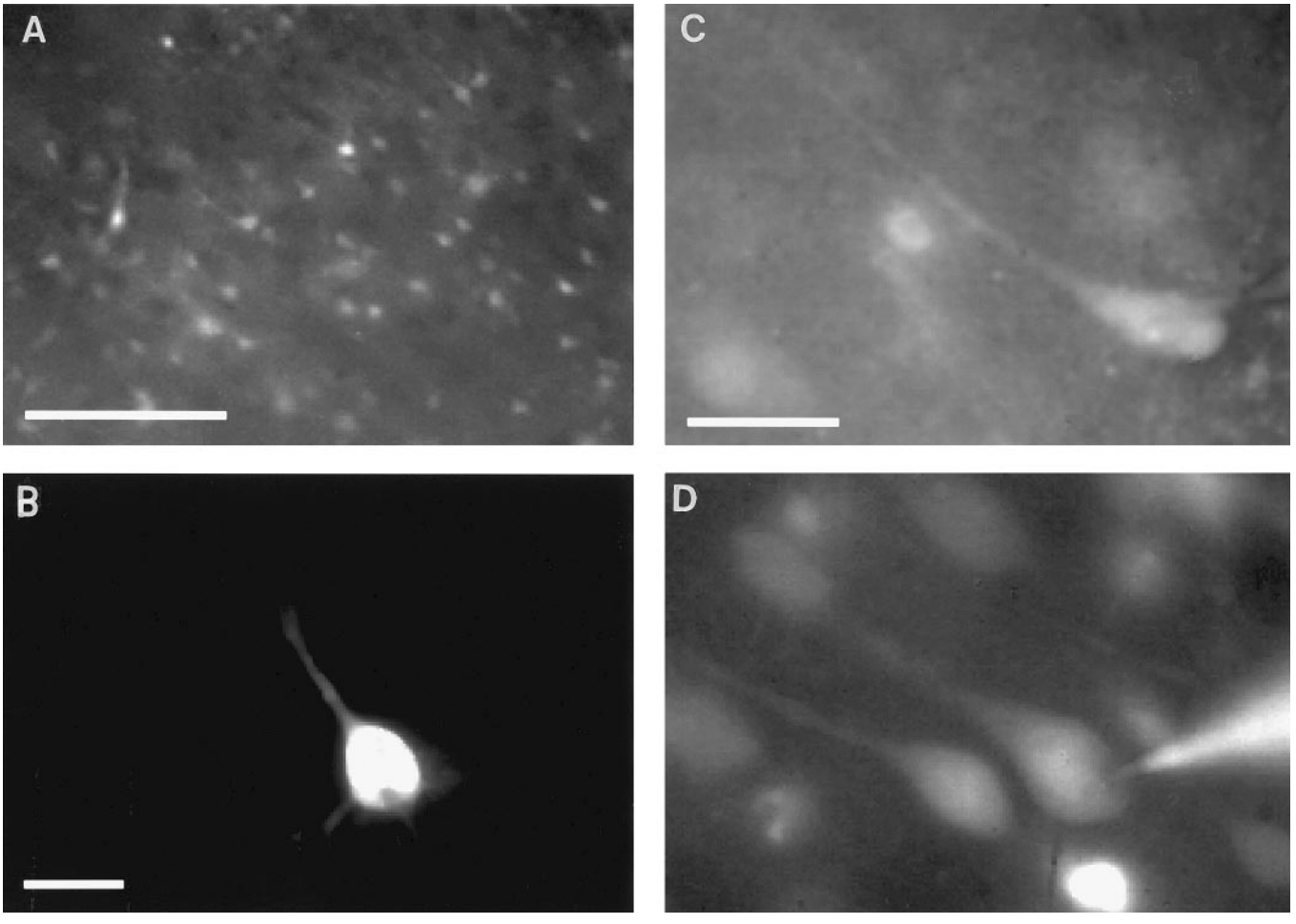

FIG. 1. Loading neocortical slices with AM indicators. (A) Fura 2-AM loading in layer 2/3 of a slice from PND 18 rat somatosensory cortex. Pial surface is up and to the left. Bar = 100 μm. Note how dozens of neurons are labeled by the indicator. (B) Layer 2/3 pyramidal neuron from a PND 13 rat loaded with 200 μM Oregon-BAPTA Green potassium salt via a patch pipet. Bar = 25 μm. Note how the apical and basal dendritic trunks are visible. (C) Perforated patch recording from a fura 2-AM loaded cell in layer 2/3 from a PND 10 animal. In some cases Fura 2-AM loading allows imaging of the largest dendrites. Bar = 25 μm. (D) Comparison of Fura 2-AM and pipet loading. Image taken from layer 2/3 of a slice from a PND 10 rat. The background cells were loaded with fura 2-AM. The central pyramidal neuron, with pipet attached, was only dimly stained before patching. The image was taken after 20 min whole-cell recording with a pipet filled with 50 μM fura-2. Bar same as in (C).

had observed that whole-cell recordings from AM loaded neurons results in a fast (1–5 min) dialysis of the Fura-2 present in the cell. Therefore, by using electrodes with a known concentration of Fura-2 we effectively clamped the Fura-2 concentration in the soma to that present in the electrode. After waiting for about 10 min for diffusional equilibrium to occur, we then imaged the filled cell and compared its fluorescence with that of other cells in the same field, loaded with Fura 2-AM (Fig. 1D). By imaging at the isosbestic excitation of 360 nm, we avoided fluorescence intensity differences that could have been produced by different resting $[Ca^{2+}]_i$. Then, using the fluorescence intensity of the reference cell as calibration, we estimated the amount of free indicator in the other cells by comparing their fluorescence intensities. These measurements were carried out with a 60×, 0.9 NA objective, and by changing the focal plane to maximize the fluorescence intensity of each cell. With this technique we estimated an intracellular concentration of indicator of approximately 25–100 μM. These values, obtained in experiments with excellent loading at PND 9–15, should be interpreted only as estimates, since their actual values will depend on many factors that affect loading, such as age, incubation time, and health of the slices.

Imaging Calcium Transients in Neurons Produced by Single Action Potentials

To characterize the calcium dynamics associated with action potentials, we first measured the fluorescence of the somata of neurons loaded with whole-cell patch pipets with known amounts potassium salts of the calcium indicators (Fig. 1B). To enable comparisons with AM loaded neurons, we carried out these experiments with low (50 μM) concentrations of dye. In response to an action potential, triggered by a current injection through the patch pipet, we observed fluorescence changes of 2–15% $\Delta F/F$ (Fig. 2A). Depolarizing pulses that did not reach threshold did not result in any calcium accumulations. The times-to-peak of these changes were approximately 5–50 ms while the decays lasted from 1 to 4 s.

To explore the calcium dynamics of neurons loaded with AM calcium indicators, we used perforated patch recording techniques to electrically record from AM loaded neurons without dialyzing their indicator (Figs. 1C, 2B). As in cells loaded with 50 μM potassium salt of indicator, AM loaded cells produced calcium transients of 2–10% $\Delta F/F$ amplitudes in response to action potentials (Fig. 2B). Their time-to-peak (around 10–40 ms) and decay kinetics (1–5 s) were also similar. The parallelism in calcium kinetics suggests that the behavior of the two different forms of indicator are similar. While this may not seem surprising, it reassures us that known problems with AM indicator loading, including incomplete deesterification, compartmentalization of the dye, and consequent changes in chemical properties of the indicator (30), did not substantially contribute to our measured signals.

Imaging Calcium Transients Produced by Trains of Action Potentials

To characterize the responses of AM loaded neurons to trains of action potentials, we carried out similar experiments, by first measuring somatic calcium kinetics in Fura-2 and Oregon-BAPTA Green loaded neurons and then comparing those measurements with those of AM loaded neurons, under perforated patch recording conditions (Fig. 3).

In neurons loaded with potassium salt of Fura-2 or Oregon-BAPTA Green, trains of action potentials

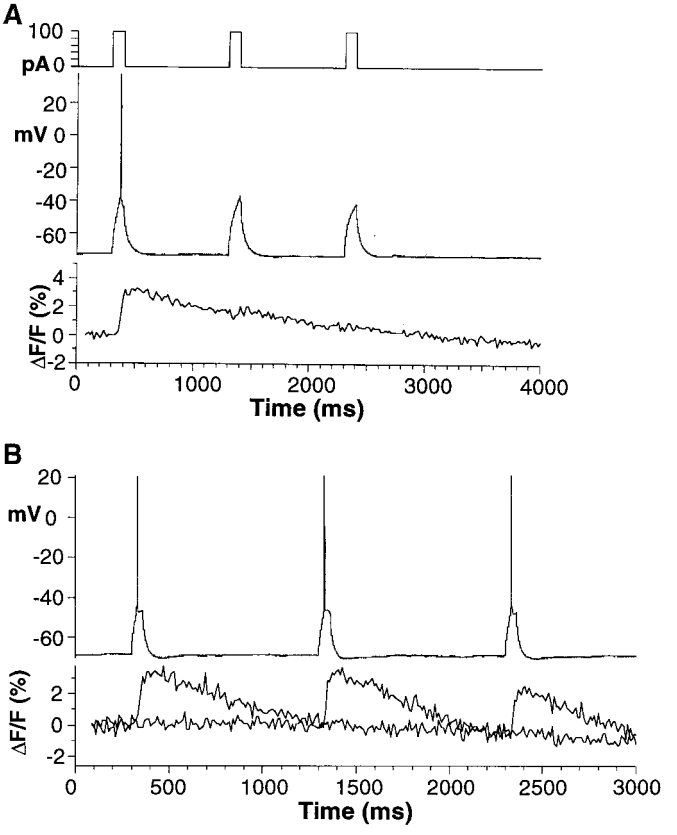

FIG. 2. Detection of individual action potentials with calcium imaging. (A) Pipet loading: Measurements from a layer 2/3 pyramidal neuron from a PND 10 rat loaded with 50 μM Fura 2-AM in the pipet. The cell was injected with three 100-pA current pulses (upper trace), and produced an action potential in response to the first stimulus (middle trace). The bottom trace shows the $\Delta F/F$ from soma. Exponential bleaching was corrected by subtracting fluorescence measured in the background region. The $\Delta F/F$ is a single trial, without smoothing. Note that the spike produces a 3% increase in the fluorescence, with a fast onset and slow decay. (B) AM loading: Similar measurements from a neuron loaded with Fura 2-AM, recorded using perforated patch. Three 60-pA current pulses were used to elicit action potentials (top trace). The bottom trace shows the $\Delta F/F$ from the soma and a background region (flat trace). Note how the amplitude and kinetics of the calcium accumulations in response to action potentials are similar to those of the neuron loaded with the potassium salt form of fura-2 with a patch pipet.

(4–50 Hz) produced cumulative calcium transients that were superimposed on top of one another (Fig. 3A). Because of the long decays associated with each spike-induced calcium transient, subsequent action potentials produced calcium accumulations that summated with the decays of the previous ones (Fig. 3A, bottom). At frequencies above 0.5 Hz, the average amplitude of the action potential-induced calcium influx was reduced as a factor of the number of previous spikes, indicating indicator saturation reached with higher $[Ca^{2+}]_i$ levels.

Neurons loaded with the AM forms of indicators also produced similar calcium kinetics in response to trains of action potentials (2–25 Hz) produced by current injections under perforated patch conditions (Fig. 3B). In the cell illustrated in Fig. 3B the perforated patch produced an unusually low access resistance, so possibly some dye washout occurred. Under presumably low

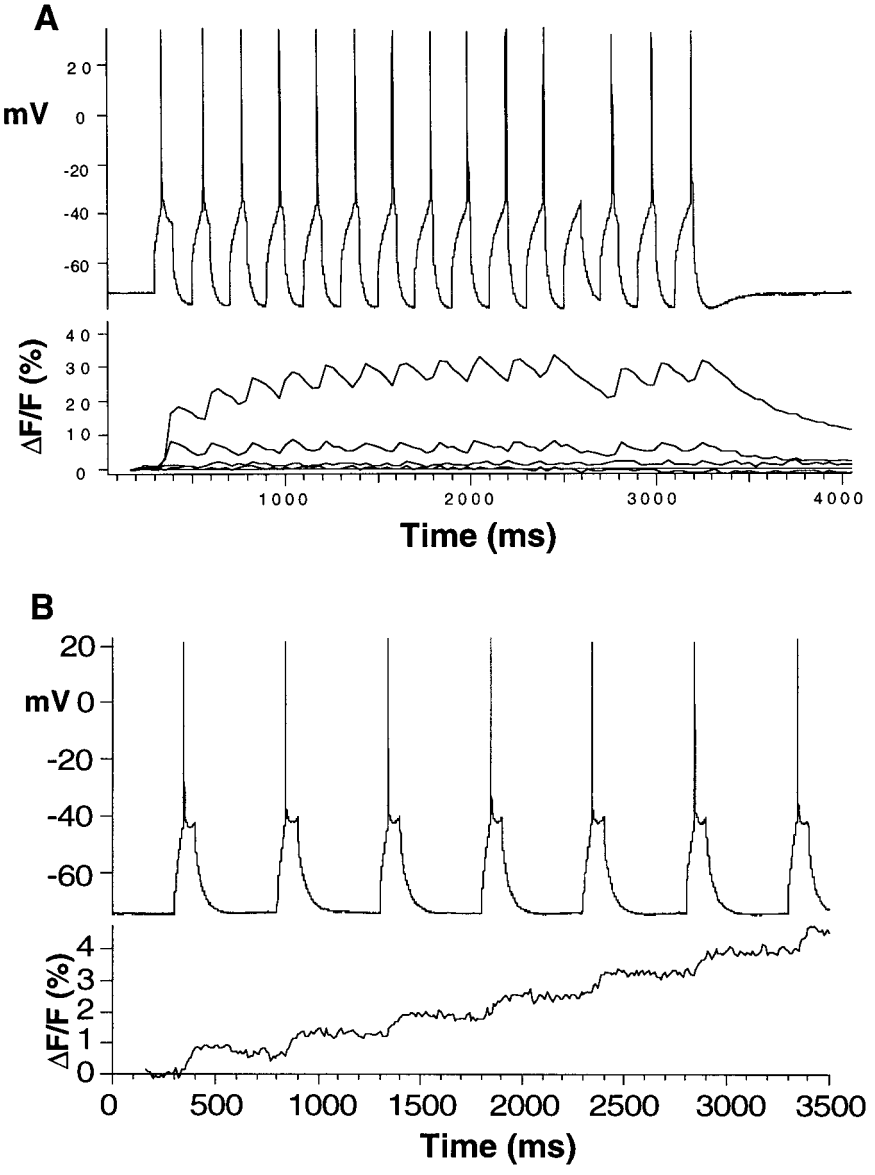

FIG. 3. Detection of trains of action potentials with calcium imaging. (A) Pipet loading: Imaging of a neuron loaded with 200 μM Oregon-BAPTA Green 1-AM potassium salt via a patch pipet. The neuron is injected with depolarizing current pulses, producing a train of action potentials at 4 Hz (top trace). The bottom shows the $\Delta F/F$ from the soma (larger trace), apical dendrite (smaller trace), and pipet and background regions (flat traces). The first spike produces a $\Delta F/F$ close to 15%, whereas the rest of the spikes produce smaller changes. Note how every spike produces a corresponding calcium accumulation. On one pulse, the cell fails to spike, showing that the calcium accumulations are due to spikes and not to the current pulses. (B) AM loading: Similar experiment on a neuron loaded with Oregon-BAPTA Green 1-AM, recorded using whole-cell patch. The cell was actually imaged during on-cell patch, but without complete washout of the AM dye. Seven spikes were elicited at 2 Hz. Note how every spike produces a corresponding calcium accumulation.

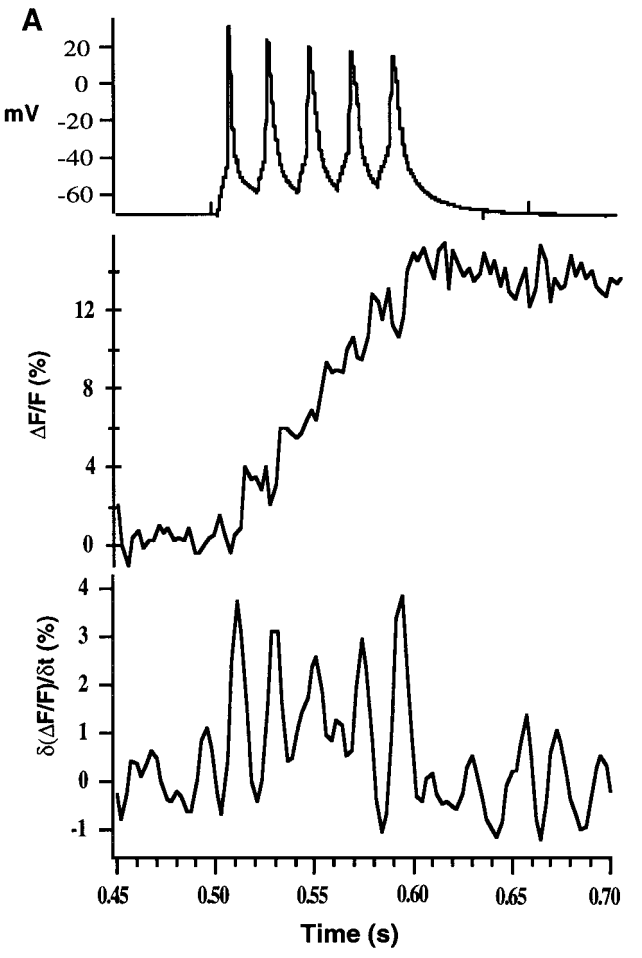

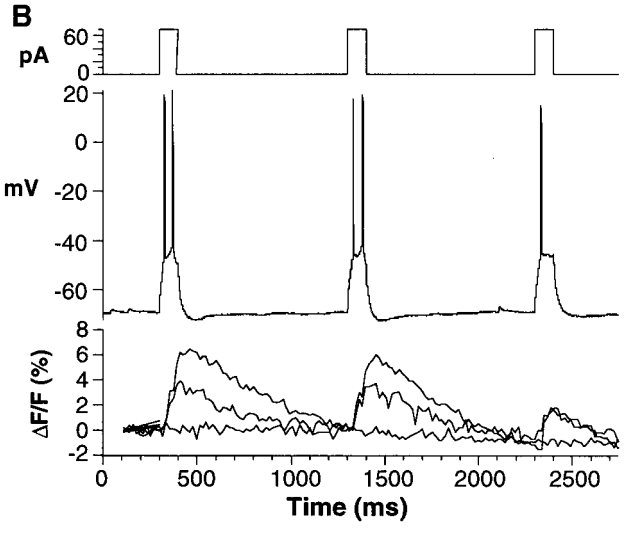

FIG. 4. Detection of high frequencies of action potential firing. (A) Pipet loading: Measurements taken from a layer 2/3 pyramidal neuron from PND 14 rat. The neuron was loaded with 100 μM Oregon-BAPTA Green 1-AM potassium salt via a patch pipet. The cell was injected with five 500-pA current pulses lasting 10 ms and fired five action potentials at 50 Hz (upper panel). The middle panel shows $\Delta F/F$ measurements from the soma, where each action potential produces a calcium accumulation. The bottom panel shows the derivative of the $\Delta F/F$. Note how each spike produces a change in the derivative that can be easily detected. Single trial, without filtering. (B) AM loading: Measurements taken from a layer 2/3 pyramidal neuron from PND 10 rat. The neuron was loaded with Fura 2-AM and recorded with perforated patch. The cell was injected with 70-pA current pulses (top panel), and fired pairs of action potentials in response to the first two pulses and a single action potential in response to the third pulse (middle panel). The bottom panel shows $\Delta F/F$ measurements from the soma, apical dendrite (middle trace), and background region (bottom trace). Linear bleaching was subtracted. The first pair of spikes are 41.5 ms apart (24 Hz), and the second pair are 51 ms apart (19.6 Hz). In the soma, the response to both spikes together is almost twice the response to a single spike (see third response), and onset of the second spike can be clearly detected. Single trial, without filtering.

dye concentration, each spike produced a calcium transient with a small amplitude (~1% $\Delta F/F$). As before, subsequent spikes produced calcium transients of lower amplitude, indicative of indicator saturation.

Detection of High Firing Frequencies with Calcium Imaging

In neurons filled with the potassium salt form of calcium indicators, we measured a time-to peak for calcium accumulations of approximately 5–50 ms. To explore the maximum frequencies of firing that we could realistically detect with calcium imaging we depolarized the neurons at different frequencies and imaged them with either the cCCD camera or a photomultiplier. For single trials, the maximum frequency at which we could reliably detect each single action potential without averaging was 50 Hz (Fig. 4A). Indeed, in those experiments it was relatively easy to reconstruct the pattern of action potential firing by thresholding the first derivative of the calcium changes (Fig. 4A, bottom). Higher frequencies produced calcium signals that were too noisy to reliably detect the onset of the accumulations associated with each spike.

In AM loaded neurons the signal-to-noise necessary for optimal reconstruction of action potentials at high frequencies was feasible only under optimal loading conditions. Figure 4B shows results from one AM loaded neuron, patched using perforated patch, where pairs of action potentials at frequencies of ~25 Hz were generated. In these experiments, the $\Delta F/F$ reflected the occurrence of each action potential, making the detection of individual spikes at 25 Hz feasible.

CONCLUDING REMARKS

In this work we sought to explore the limits of action potential detection as a function of spike frequency. Our strategy was to concentrate on detecting the on-

sets of the calcium accumulations, which are produced by the opening of calcium channels that occurs during the action potential (31). The onset kinetics of the fluorescent signals depends on the calcium kinetics, influenced by the geometry of the cell, and on the diffusional and buffering properties of calcium, as well as on the rate constants of the indicators. In experiments imaging spike-induced calcium transients in dendritic shafts and spines we had previously found that the spike-induced calcium accumulations had times-to peak of less than 2 ms, which was the time resolution of our measurements (24). This would in principle produce an upper bound limit of approximately 500 Hz to the detection of firing frequencies in dendrites. Nevertheless, in neuronal somata we now measure much slower onset times, probably because of the diffusional delays associated with the smaller surface-to-volume ratio of the soma. In our experiments we could detect firing rates of up to 50 Hz without averaging, and we suspect that the diffusional delays will limit this approach to detecting frequencies of up to 100 Hz, which seems appropriate for optimal recording from most classes of neurons.

ACKNOWLEDGMENTS

We thank S. Cash, M. López de Armentia, and V. Unni for their help. This work was supported by the Epilepsy Foundation of America and the March of Dimes, Klingestein, EJLB, and Beckman foundations and by the National Institutes of Health (EY 111787-01A1).

REFERENCES

1. Heiligenberg, W. (1991) *Neural Nets in Electric Fish*, MIT Press, Cambridge, MA.
2. Konishi, M. (1990) *Cold Spring Harbor Symp. Quant. Biol.* **55,** 575–584.
3. Hubel, D. H., and Wiesel, T. N. (1977) *Proc. R. Soc. London B* **198,** 1–59.
4. Hopfield, J. J. (1982) *Proc. Natl. Acad. Sci. USA* **79,** 2554–2558.
5. Hopfield, J. J., and Tank, D. W. (1986) *Science* **233,** 625–633.
6. Gerstein, G. L., Bedenbaugh, P., and Aertsen, M. H. (1989) *IEEE Trans. Biomed. Eng.* **36,** 4–14.
7. Meister, M., Wong, R. O. L., Baylor, D. A., and Shatz, C. J. (1991) *Science* **252,** 939–943.
8. Sterling, P. (1990) *in* The Synaptic Organization of the Brain (Shepherd, G. M., Ed.), Oxford Univ. Press, Oxford.
9. Cohen, L. (1989) *in* Annual Review of Physiology (Hoffman, J. F., and De Weer, P., Eds.), pp. 487–582, Annual Review Inc., Palo Alto, CA.
10. Cohen, L. B., and Keynes, R. D. (1971) *J. Physiol.* **212,** 259–275.
11. Lipton, P. (1973) *J. Physiol.* **231,** 365–383.
12. Cohen, L. B., and Lesher, S. (1986) *in* Optical Methods in Cell Physiology (De Weer, P., and Salzberg, B. M., Eds.), pp. 72–99, Wiley–Interscience, New York.
13. Tsien, R. Y. (1989) *Annu. Rev. Neurosci.* **12,** 227–253.
14. Grinvald, A., Manker, A., and Segal, M. (1982) *J. Physiol.* **333,** 269–291.
15. Grinvald, A., Lieke, E. E., Frostig, R. D., and Hildesheim, R. (1994) *J. Neurosci.*
16. Grinvald, A., Ross, W. N., and Farber, I. (1981) *Proc. Natl. Acad. Sci. USA* **78,** 3245–3249.
17. Yuste, R., Tank, D. W., and Kleinfeld, D. (1997) *Cereb. Cortex* **6/7,** 546–558.
18. Yuste, R., and Katz, L. C. (1989) *Soc. Neurosci. Abstr.* **4.5,** 2.
19. Yuste, R., and Katz, L. C. (1991) *Neuron* **6,** 333–344.
20. Cornell-Bell, A. H., Finkbeiner, S. M., Cooper, M. S., and Smith, S. J. (1990) *Science* **247,** 470–473.
21. O'Donovan, M. J., Ho, S., Sholomenko, G., and Yee, W. (1993) *J. Neurosci. Methods* **46,** 91–106.
22. Tank, D. W., Sugimori, M., Connor, J. A., and Llinás, R. R. (1988) *Science* **242,** 773–777.
23. Delaney, K. R., Zucker, R. S., and Tank, D. W. (1989) *J. Neurosci.* **9,** 3558–3567.
24. Yuste, R., and Denk, W. (1995) *Nature* **375,** 682–684.
25. Tsien, R. Y. (1981) *Nature* **290,** 527–528.
26. Yuste, R., Gutnick, M. J., Saar, D., Delaney, K. D., and Tank, D. W. (1994) *Neuron* **13,** 23–43.
27. Helmchen, F., Imoto, K., and Sakmann, B. (1996) *Biophys. J.* **70,** 1069–1081.
28. Tank, D. W., Delaney, K. D., and Regehr, W. G. (1996) *J. Neurosci.*
29. Yuste, R. (1999) *in* Imaging Living Cells (Konnerth, A., Lanni, F., and Yuste, R., Eds.), Cold Spring Harbor Press, Cold Spring Harbor, NY.
30. Williams, D. A., and Fay, F. S. (1990) *Cell Calcium* **11,** 75–84.
31. Llinas, R., Steinberg, I. Z., and Walton, K. (1976) *Proc. Natl. Acad. Sci. USA* **73,** 2913–2922.